
Interactions Between Sodium Ion and Constituents of Chitosan: DFT Study

Marwa Emmanuel^{1,2,*}, Alexander Pogrebnoi^{1,2}, Tatiana Pogrebnyaya^{1,2}

¹The Nelson Mandela African Institution of Science and Technology (NM-AIST), Arusha, Tanzania

²Dept. of Materials, Energy Science and Engineering, The NM-AIST, Arusha, Tanzania

Email address:

marwaking39eti@gmail.com (M. Emmanuel), marwae@nm-aist.ac.tz (M. Emmanuel), alexander.pogrebnoi@nm-aist.ac.tz (A. Pogrebnoi), pgamtp@mail.ru (A. Pogrebnoi), tatiana.pogrebnyaya@nm-aist.ac.tz. (T. Pogrebnyaya)

To cite this article:

Marwa Emmanuel, Alexander Pogrebnoi, Tatiana Pogrebnyaya. Interactions Between Sodium Ion and Constituents of Chitosan: DFT Study. *International Journal of Materials Science and Applications*. Vol. 4, No. 5, 2015, pp. 303-313. doi: 10.11648/j.ijmsa.20150405.15

Abstract: Glucosamine and acetylglucosamine are the constituents of chitosan and chitin natural biopolymers. In the present study, the structure and properties of the D-glucosamine monomer (A), N-acetylglucosamine monomer (B), and ion-molecular adducts with Na⁺ cation have been explored. The equilibrium geometrical structure, vibrational spectra of the species have been determined, using the DFT/B3LYP method with the 6-31G(d) basis set. Larger basis sets up to 6-311++G(d,p) were utilized to compute energies of reactions between Na⁺ ion and A and B molecules. The exothermicity and spontaneous character of the adducts formation reactions have been confirmed.

Keywords: B3LYP, Glucosamine, Acetylglucosamine, Adduct, Geometrical Structure, Vibrational Spectrum, Energy and Enthalpy of Reaction

1. Introduction

Glucosamine (C₆H₁₃NO₅) is a bioactive amino monosaccharide which is a precursor for the synthesis of important macromolecules known as building blocks of the joint cartilage and connective tissues, contributing to their strength and flexibility. Glucosamine belongs to amino sugar group which is well-known precursor in the biochemical synthesis of glycosylated proteins and lipids [1, 2, 3]. Being part of the structure of the polysaccharides chitosan and chitin compose the exoskeletons of crustaceans and other arthropods, as well as the cell walls of fungi and many higher organisms [4, 5, 6]. Chitosan is an unbranched cationic biopolymer, the derivative of chitin (N-acetyl glucosamine) [7, 5]. It is produced commercially by the hydrolysis of crustacean exoskeletons [4-6, 8] or, less commonly, by fermentation of a grain such as corn or wheat. Glucosamine appears to be harmless for use as a dietary supplement [8, 9]. Chitosan as a biopolymer is important in assorted pharmaceutical, biomedical [4] biotechnological [10] applications and in drinking water and waste water treatment [9, 11, 12] owing to its ability to remove metallic ions [11]. Chitosan has three types of reactive functional groups, which are amino groups, hemiacetal groups, and hydroxyl groups [13-16] which allow

further chemical modification and let it to be an ideal cation exchanger [17, 18]. Specific application of chitin and chitosan is openly linked to their physical chemical properties [8, 13, 14].

Acetylglucosamine is a monosaccharide derivative of glucose it is an amide between glucosamine and acetic acid [1]. It is part of a biopolymer in the bacterial cell wall, built from alternating units of N-acetyl glucosamine and N-acetylmuramic acid cross-linked with oligopeptides at the lactic acid residue of N-acetylmuramic [3].

Accurate predictions of molecular structures, reactivities, vibrational, electronic and NMR spectra can be obtained by means of quantum chemical calculations. DFT is presently the most successful (and also the most promising) approach to compute the electronic structure of matter. Its applicability ranges from atoms, molecules, solids to nuclei, quantum and classical fluids [19]. Enthralling facet of DFT is that even the simplest systems can show intricacies and challenges reflecting those of much larger and complex systems [20]. Taking advantage of readily accessible theoretical tools, a lot of studies have been done in predicting molecular structure, interactions and properties and in the long run helps to understand chemical reactions.

The aim of the present work is to explore the interactions of chitosan constituents, glucosamine and acetylglucosamine,

with sodium ion. It is well known that glucosamine molecule may exist in different conformers, chair, boat and staggered conformation [1], among which, chair conformer being the most stable form and has the lowest energy [21]. Moreover for the chair conformer, α -D-Glucosamine, several modifications have been reported [21]. One of the glucosamine conformers has been studied previously in [22]. In the present work, the molecule of glucosamine is denoted as A and acetylglucosamine as B. For the former two conformers are considered: the first one is the same as studied in [22] and denoted hereafter as A_X and second one is A_Y . These two modifications differ by mutual position of the OH and NH_2 groups regarding the ring.

2. Computational Details

The quantum chemical study of glucosamine, acetyl glucosamine molecules and their respective adducts with sodium ion has been done using DFT with Becke-Lee-Yang-Parr functional (B3LYP) [19, 20]. Optimization of geometrical parameters and the vibrational spectra computation were performed under polarized split-valence basis set 6-31G(d), and the larger basis sets up to 6-311++G(d,p) were utilized to compute energies of interaction of Na^+ ion with glucosamine and acetylglucosamine molecules. The Firefly quantum chemical package, version 8.1.0 [23] partially based on the GAMESS (US) source code [24] has been employed.

Initial construction of molecules and adducts at large was obtained using HyperChem quantum chemical package [25], the coordinates obtained were used in Firefly for further optimization. The minima of energies were proved by the absence of imaginary frequencies in the vibrational spectra. For visualization of the optimized structures, specification of geometrical parameters and vibrational modes, the wxMacMolplot [26] and Chemcraft [27] softwares have been used.

In this item geometrical parameters and vibrational frequencies are given as found using 6-31G(d) bases set; while charges on atoms and energies of reactions are given as found using 6-311++G(d,p) bases set.

3. Results and Discussion

3.1. Geometrical Structure

3.1.1. Glucosamine A and ANa^+ Adducts

Glucosamine and acetylglucosamine molecules may exist in linear or cyclic forms; the latter being the most stable and favored form [1, 28, 29]. Different cyclic conformers have been identified [1, 21]. In the current study conformer α -D-Glucosamine (A_Y) have been considered and compared to conformer reported in [22] (A_X), the rundown of A_Y and A_X are presented in Tables 1 and 2, respectively.

In both species the ring is held together by the oxygen atom inserted between carbon atoms. The ring is not planar as the sum of valence angles is less than 720° , and also the

values of torsion angles confirm non-planarity. Both configurations considered are close to conformer denoted as α -G-g+/cc/t in [21] and belong to 4C_1 chair conformer of α -D glucosamine with slight different orientation of hydroxyl groups. After optimization procedure done using 6-31G(d) bases set it appeared that the total energy of the conformer A_Y is ~ 39 kJ \cdot mol $^{-1}$ lower than that of A_X .

The equilibrium structures for A_Y conformer and the adduct A_YNa^+ are presented in Fig. 1 (a), (b); the selected geometrical parameters and atomic charges are given in Table 1. In A_Y molecule three hydroxyl groups are linked to the carbon atoms of the ring, and are located at the same side of the ring as the NH_2 -group, in the adduct A_YNa^+ , two hydroxyl groups remain at the same side but the third OH-group is turned over the ring and forms the hydrogen bond O12-H24...O9.

In monomer A_Y the oxygen atom of the ring is inserted between C4 and C7 making an angle C4-O1-C7 equal to 115° and the bond lengths are 1.441 and 1.402 Å. In the A_YNa^+ complex, the C7-O8-C4 valence angle is 116° and the bond lengths are 1.441 and 1.391 Å for C4-O8 and C7-O8 respectively. Thus attachment of Na^+ to the A_Y molecule has no significant change to the geometry of the C-O-C ring fragment. The Na^+ ion approaches atoms O10, O11, and N13 which have most negative charges, -0.33, -0.38 and -0.46, respectively (Table 1). Nitrogen being more negatively charged, dictates the position of the Na^+ attachment. Thus three bonds are formed within the A_YNa^+ complex, these bonds together with hydrogen bond attributes to the stability of this adduct.

In A_X monomer, Fig. 2 (a), the oxygen atom of the ring is between C4 and C5 making an angle C5-O7-C4 equal to 114° and the bond lengths C5-O7 and C4-O7 are 1.431 and 1.414 Å, respectively. In the A_XNa^+ complex, Fig. 2 (b), in the similar C5-O7-C4 fragment the valence angle is 119° and the C5-O7 and C4-O7 bond lengths are 1.455 and 1.411 Å, respectively. Thus the attachment of Na^+ to A_X molecule brings a slight change to the geometry of the molecule A_X and the C-O-C angle increases with Na^+ attachment. It is seen that in A_X , one hydroxyl group, linked to the carbon atom of the ring, is located at the same side of the ring as the NH_2 -group while two hydroxyl groups are in opposite side of the ring. In the adduct A_XNa^+ , two hydroxyl groups remain at the opposite sites of the ring and O1-H22 in the same side with NH_2 -group attaches Na^+ .

Contrary to A_Y , Na^+ ion doesn't attach to nitrogen but rather approaches O1 from hydroxyl group and O7 from the ring whose respective charges are -0.16 and -0.04 (Table 2). Apparently the position of Na^+ attachment is determined by not only the atomic charges but also the steric factors (mutual position of the atoms interacting). At this juncture two bonds are formed within A_XNa^+ adduct which is O1... Na^+ and O7... Na^+ contrary to A_YNa^+ , where three bonds are formed. Comparing the energies of A_XNa^+ and A_YNa^+ of two adducts calculated in 6-311++G(d,p) basis set, the total energy of the adduct A_YNa^+ is ~ 72 kJ \cdot mol $^{-1}$ lower than that of A_XNa^+ . Therefore, both species, A_Y and A_YNa^+ are energetically more

stable than A_X and A_XNa^+ , respectively.

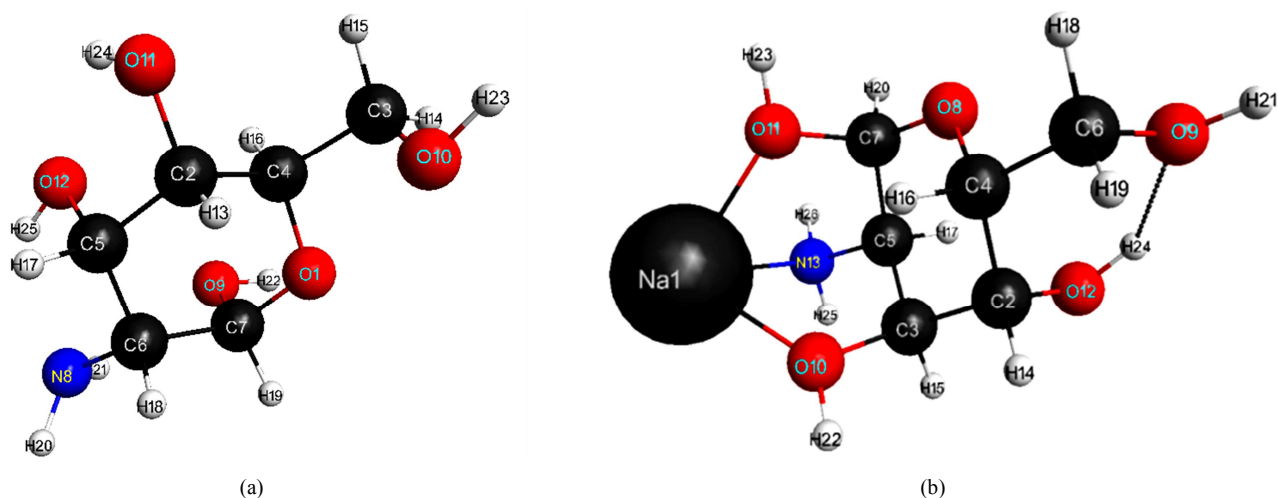


Figure 1. Equilibrium geometrical structure of the species: A_Y (a); A_YNa^+ (b).

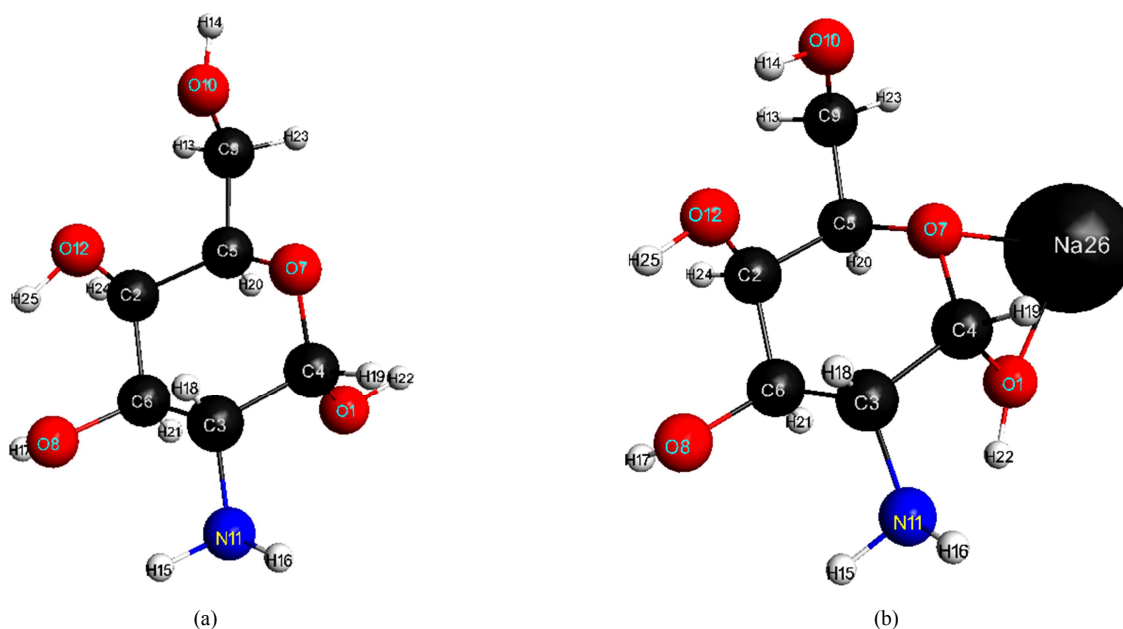


Figure 2. Equilibrium geometrical structure of the species: A_X (a); A_XNa^+ (b).

Table 1. Selected geometrical parameters and atomic charges of the glucosamine molecule A_Y , and A_YNa^+ adduct.

Species	Internuclear distance, Å		Valence angle, Deg		Torsion angle, Deg		Atom	Charge, a.u
A_Y	C5-O12	1.421	O12-C5-C6	110.4	O12-C5-C6-N8	-45.3	O9	-0.20
	C6-N8	1.475	N8-C6-C7	111.8	N8-C6-C7-O9	41.4	O10	-0.25
	C7-O9	1.419	O9-C7-O1	112.6	O9-C7-O1-C4	65.9	O11	-0.15
	C4-O1	1.441	C4-O1-C7	115.0	C4-O1-C7-C6	-56.7	O12	-0.20
	C7-O1	1.402	O1-C7-C6	112.7	O1-C7-C6-N8	166.5	N8	-0.30
	C3-O10	1.424	O10-C3-C4	109.5	O10-C3-C4-C2	58.0	O1	-0.04
A_YNa^+	C3-O10	1.443	C3-O10-Na1	112.7	C3-O12-Na1-N13	20.0	O9	-0.31
	C5-N13	1.481	C5-N13-Na1	95.9	C5-N13-Na1-O11	44.2	O10	-0.33
	C7-O8	1.391	C7-O8-C4	115.9	C7-O8-C4-C2	58.1	O11	-0.38
	O12-C2	1.406	O12-C2-C4	114.2	O12-C2-C4-C6	-61.7	O12	-0.15
	O9-C6	1.425	O9-C6-C4	109.3	O9-C6-C4-O8	-70.8	N13	-0.46
	C4-O8	1.441	C4-O8-C7	116				
	O9.H24-O12	3.957					Na+	0.79

Note: Here and in Tables 2 and 3, the bolded numbers represent charges for the most negatively charged atoms where Na^+ attachment take place.

Table 2. Selected geometrical parameters and atomic charges of the glucosamine molecule A_X and A_XNa^+ adduct.

Species	Internuclear distance, Å		Valence angle, Deg		Torsion angle, Deg		Atom	Charge, a.u
A_X	O1-C4	1.411	O1-C4-O7	112.0	O1-C4-O7-C5	62.6	O1	-0.16
	C4-O7	1.414	C4-O7-C5	114.0	C4-O7-C5-C2	57.7	C4	-0.57
	C5-O7	1.431		114.0			O7	-0.04
	O12-C2	1.412	O12-C2-C6	109.6	O12-C2-C6-O8	46.6	O8	-0.27
	O8-C6	1.441	O8-C6-C3	106.9	O8-C6-C3-N11	63.2	C9	-0.44
			O1-C4-C3	109.2	O1-C4-C3-N11	55.2	O10	-0.22
	O10-C9	1.413	O10-C9-C5	111.5	O10-C9-C5-C2	67.6	N11	-0.27
	O9...H24-O12						O23	-0.12
A_XNa^+	O1-C4	1.431	O1-C4-O7	107.2	O1-C4-O7-C5	84.3	O1	-0.33
	C4-O7	1.411	C4-O7-C5	119.0	C4-O7-C5-C2	44.8	C4	-0.22
	C5-O7	1.455					O7	-0.12
	O12-C2	1.418	O12-C2-C6	110.6	O12-C2-C6-O8	54.0	O8	-0.22
	O8-C6	1.426	O8-C6-C3	106.1	O8-C6-C3-N11	71.6	C9	-0.44
	O1-C4	1.431	O1-C4-C3	109.5	O1-C4-C3-N11	38.9	O10	-0.14
	O10-C9	1.400	O10-C9-C5	114.0	O10-C9-C5-C2	72.0	N11	-0.34
							O23	-0.19
						Na+	0.84	

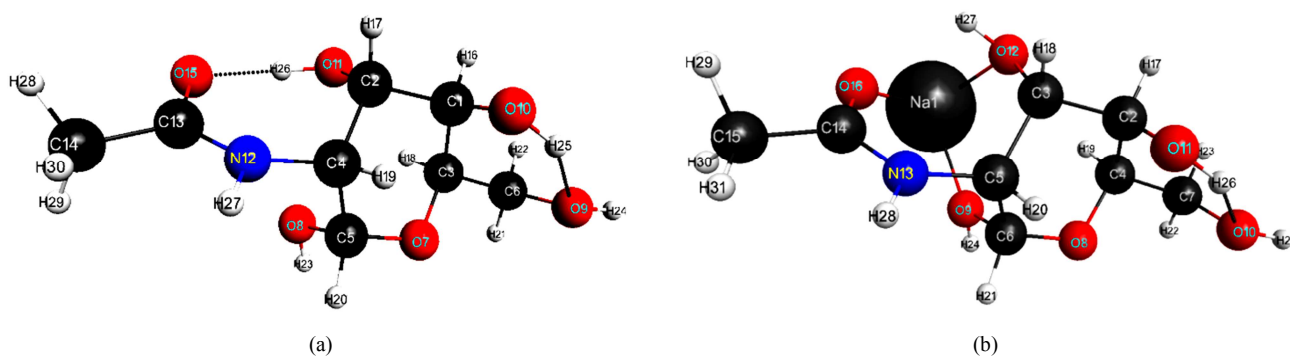
3.1.2. Acetylglucosamine B and BNa^+ Adduct

The selected parameters of acetylglucosamine B and BNa^+ adduct are given in Table 3; the structures are shown in Fig. 3. The geometrical parameters of B do not differ remarkably compared to A. The C-O-C geometrical parameters for B conformer are similar to those of A_Y and A_X as the C3-O7-C5 angle of the ring is 115° and bond lengths C3-O7 and C5-O7 are 1.438 Å and 1.413 Å, respectively. However worth to note, two hydrogen bonds are formed in monomer B, O11-H26...O15 and O10-H25...O9, Fig. 3 (a) which is contrary to A_X where no H-bonds exist and A_Y where one H-bond exists. In the molecule B presence of acetyl group which is bound to the nitrogen atom changes the electron charge distribution in the vicinity: nitrogen atom gains positive charge $q = 0.07$ contrary to A_Y and A_X where nitrogen is negatively charged, $q = -0.30$ and -0.27 respectively. This is accredited to the presence of oxygen in

the acetyl group which draws electron from nitrogen and creates electron deficiency at its periphery.

In the BNa^+ adduct, the sodium ion attaches to three negatively charged oxygen; two atoms in the ring (O9, O12) and one (O16) in the acetyl-group. This distinguishes adduct BNa^+ from A_YNa^+ where the bonds are between $Na^+...O10$, $Na^+...O11$ and $Na^+...N13$, and A_XNa^+ where the bonds are formed between $Na^+...O7$ atoms of the ring and $Na^+...O1$ atom from hydroxyl group. Actually Na^+ ion attaches at nucleophilic sites in both molecules A_X , A_Y and B to form adducts.

In BNa^+ there is one hydrogen bond as seen in Fig. 3 (b), between O11-H26...O10. When Na^+ approaches acetylglucosamine molecule which has two H-bonds (O10-H25...O9 and O11-H26...O15), one of them in the nitrogen vicinity is broken. The other H-bond in the opposite side of the ring is left unchanged as in B.

**Figure 3.** Equilibrium geometrical structure of the species: B (a); BNa^+ (b).**Table 3.** Selected geometrical parameters and atomic charges of the glucosamine molecule B and BNa^+ adduct.

Species	Internuclear distance, Å		Valence angle, Deg		Torsion angle, Deg		Atom	Charge, a.u
B	C4-N12	1.468	C4-N12-C13	129.4	C4-N12-C13-O15	-11.0	O7	-0.03
	O15...H26	1.638					O8	-0.17
	C3-O7	1.438	C3-O7-C5	115				
	C5-O7	1.413						
	O9.H25-O10	4.307					O9	-0.31
	O8-C5	1.406	O8-C5-O7	113.0	O8-C5-O7-C3	70.3	O10	-0.17

Species	Internuclear distance, Å	Valence angle, Deg	Torsion angle, Deg	Atom	Charge, a.u			
BNa ⁺	O11-C2	1.404	O11-C2-C1	105.9	O11-C2-C1-O10	169.6	O11	-0.17
	C13-O15	1.500					O15	-0.33
	O11-H26.O15	4.105						
	C2-O11	1.404					N12	0.07
	O9-C6	1.434	O9-C6-C3	110.0	O9-C6-C3-O7	-68.4	C6	-0.81
	O9-Na1	2.230	C6-O9-Na1	125.9	C6-O9-Na1-O16	-58.6	Na1	0.69
	O16-Na1	2.199					O8	0.04
	O12-Na1	2.325	O9-Na1-O12	86.9	C6-O9-Na1-O12	16.5	O9	-0.32
	O12-C3	1.439	C3-O12-Na1	121.2	C5-C3-O12-Na1	-12.1	O10	-0.30
	N13-C14	1.356	N13-C14-O16	123.7	N13-C14-O16-Na1	35.0	O11	-0.12
	O16-C14	1.244	O9-Na1-O16	91.3	O9-Na1-O16-C14	7.3	O12	-0.15
	C6-O8	1.393						
	O10...H26-O11	1.840		143.0			N13	0.04
	C4-O8	1.442	C4-O8-C6	116.4			O16	-0.44

3.2. Vibrational Spectra

Table 4. Vibrational spectra ranges (in cm^{-1}) for glucosamine, acetylglucosamine and adducts with Na⁺.

Species	1st region	2nd region	3rd region
A _Y	60-1670	2960-3120	3510-3780
A _Y Na ⁺	70-1690	2960-3090	3450-3800
A _X	60-1690	2910-3100	3480-3760
A _X Na ⁺	50-1700	2980-3060	3360-3750
B	60-1770	2990-3160	3450-3800
BNa ⁺	50-1730	3010-3160	3620-3800

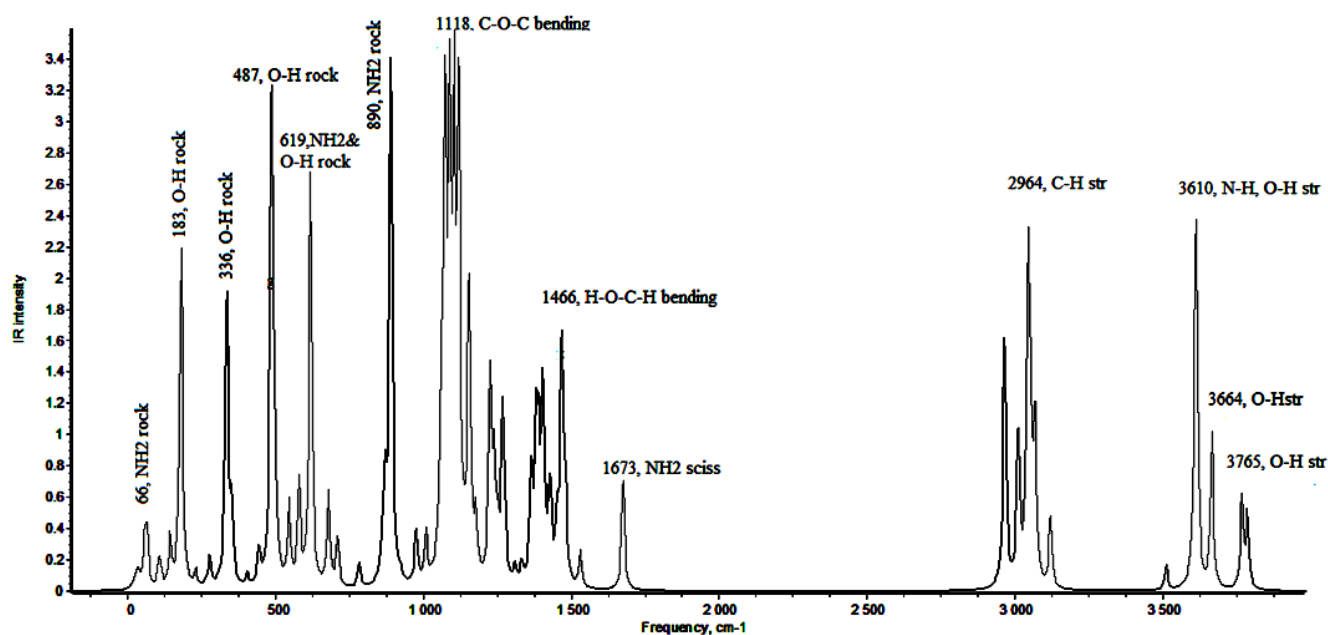
The vibrational spectra of glucosamine molecules and their adducts with sodium ion were computed for the optimized structures, the absence of imaginary frequencies proved the structures to be at equilibrium. Scrutiny of the outputs exposed existence of three regions with significant absorption intensities per each molecule and respective adducts (Table 4). As is seen, for all six species these regions are very similar. The IR spectra are shown in Figs. 4-6. As the symmetry of the species is low (C_1), all vibrational modes are active in IR

spectra and have non-zero intensities. The characteristic vibrational modes have been considered vis-à-vis the functional groups.

A_Y. The great majority of the frequencies are manifested in the first low frequency region and include mostly the rocking modes of NH₂ and OH groups and bending vibrations of the ring. The most intensive mode of 1118 cm^{-1} relates to the C-O-C bend vibration. In the high frequency regions, the stretching modes of C-H, N-H and O-H groups are observed.

A_YNa⁺. In the Na⁺-adduct, the stretching and bending modes of the fragment O-Na-N appear in the low frequency region. The complicated bending vibration involving the O-Na-N fragment together with O-H...O group corresponds to the frequency of 369 cm^{-1} . The most intensive vibrations in the adduct relate to the bending of the C-O-C fragment (1018 cm^{-1}) and also stretching O-H...O (3630 cm^{-1}) and rocking mode (584 cm^{-1}) of the hydrogen bond.

A_X. The most intensive vibrations correspond to rocking of O-H group (544 cm^{-1}), and asymmetrical stretching of the C-O-C bond of the ring (1076 cm^{-1}) have been appreciably noticed.



(a)

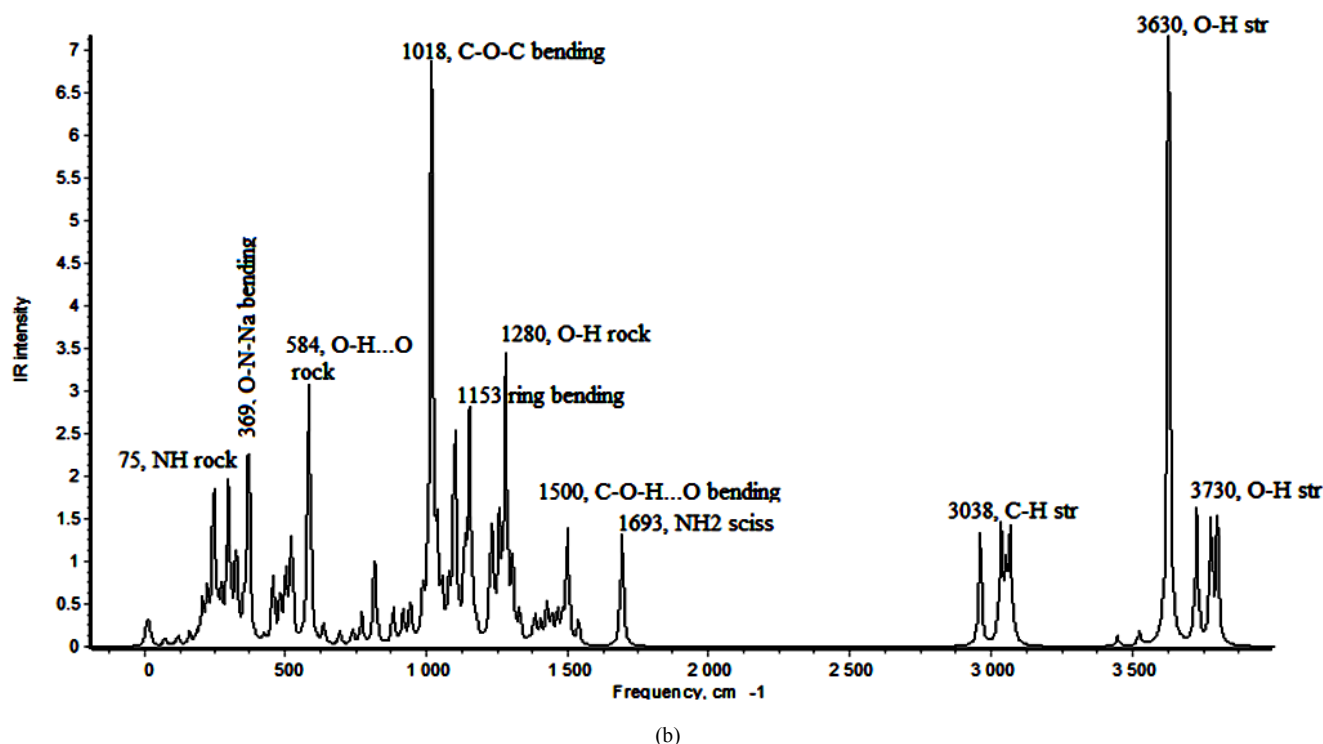


Figure 4. Theoretical IR spectra of glucosamine molecule A_Y (a) and adduct A_YNa^+ (b).

A_XNa^+ . In the A_XNa^+ adduct the red shift (compared to A_X) of the most intensive vibrations is observed. In the first region, the band 494 cm^{-1} corresponds to the combination of OH group rocking and bending of the ring; 972 cm^{-1} is the stretching mode of C-O, NH_2 wagging and bending of the ring as well. In the higher frequency region, the intensive band appeared at 3365 cm^{-1} , it is the stretching mode of OH-bond linked with Na^+ atom.

B. Two hydrogen bonds are displayed through very intensive antisymmetrical stretching modes: 3449 cm^{-1} assigned to the hydrogen bond related to the acetyl group and 3677 cm^{-1} caused by the second hydrogen bond of the molecule. The wagging vibrations of hydrogen bonds are seen in the low frequency region as well: 529 cm^{-1} and 691 cm^{-1} . The stretching modes related to acetyl groups manifest in the bands of 1582 (C-N) and 1768 cm^{-1} (C=O). The high intensity peak at 1091 cm^{-1} corresponds to the asymmetrical stretching vibration of the C-O-C fragment of the ring.

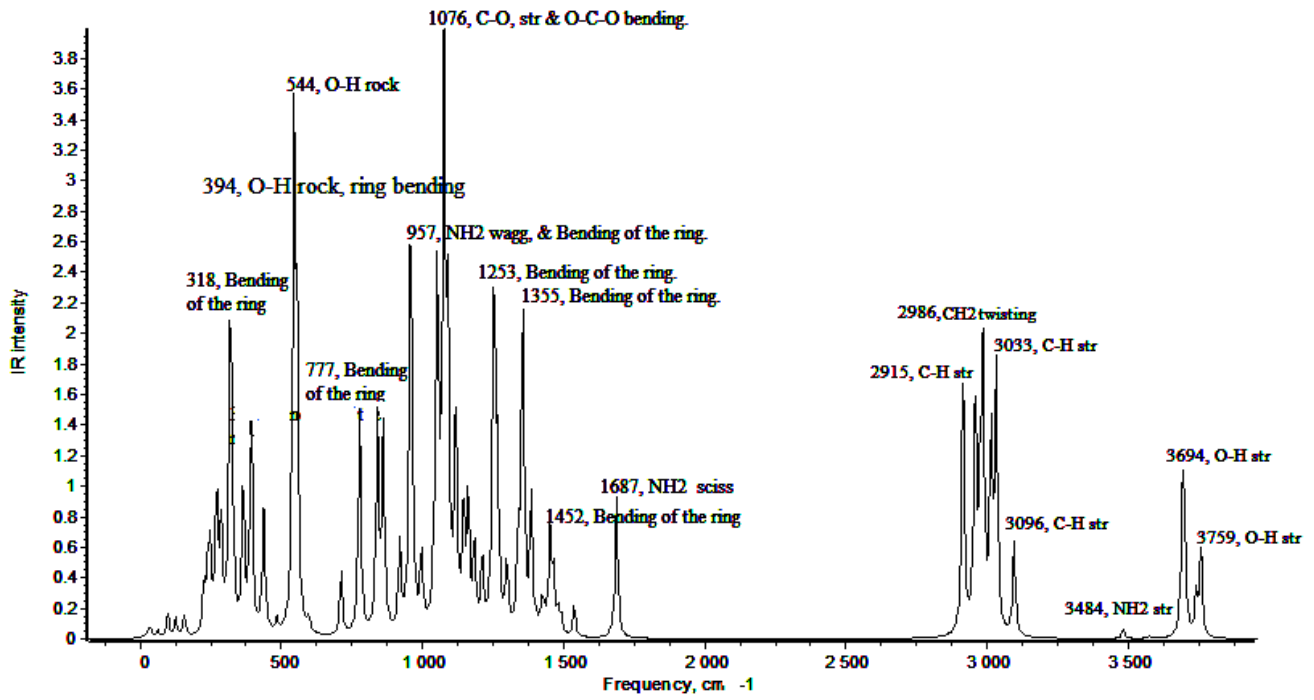
BNa^+ . Similar to the glucosamine molecule, the most intensive vibration in the adduct is the stretching vibration (3624 cm^{-1}) of the hydrogen bond related to the acetyl group, but shifted to higher frequency. The second hydrogen bond existed in the B molecule, is not any more in the adduct thus the corresponding peak (observed in B, 3677 cm^{-1}) is absent in the high frequency region in the spectrum of BNa^+ .

Concluding the discussion about theoretical vibrational spectra of the species some similar features may be noted due to the similarity of the structures: the existence of three regions of frequencies, and the broad first range; the bands of high intensities due to the C-O-C fragment of the ring, and

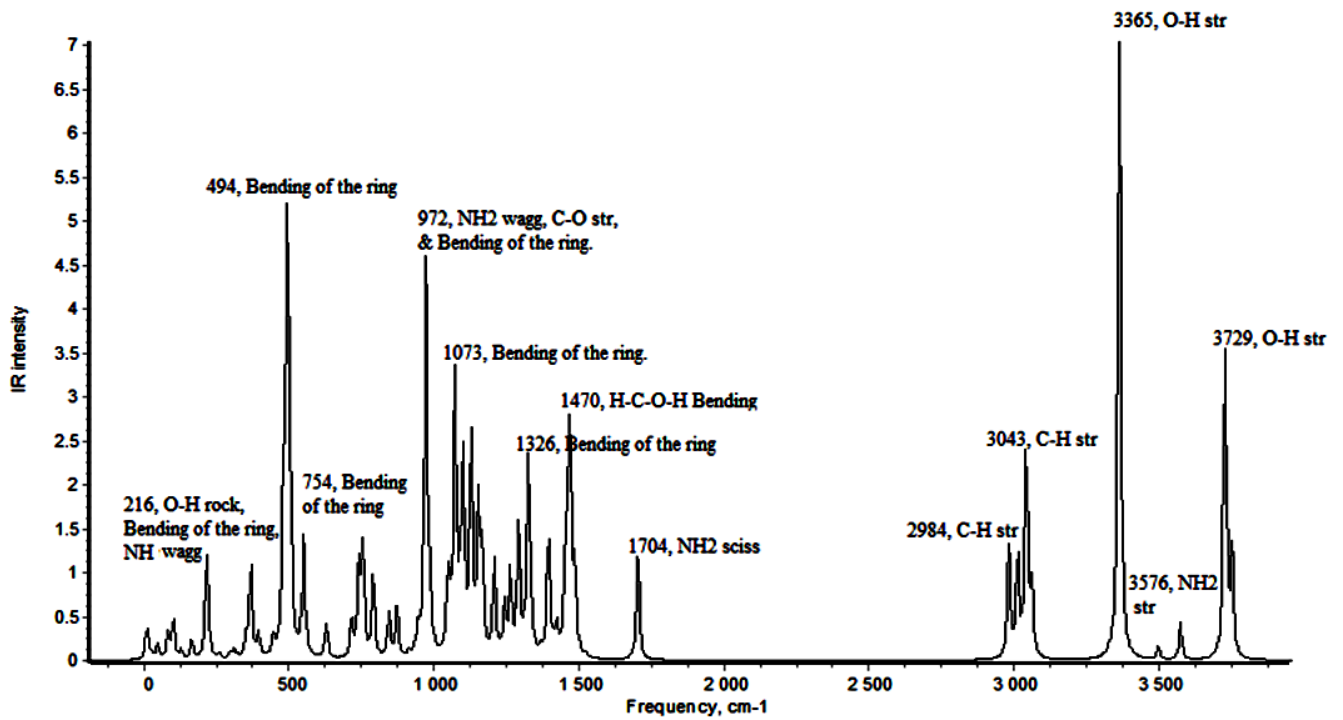
OH stretching vibrations. In A_YNa^+ , B and BNa^+ , the formation of hydrogen bonds lead to the noticeable increase of the IR intensities of the OH stretching modes. In the adducts, the sodium atom is involved into low frequency vibrations, less than 370 cm^{-1} of low IR intensities.

As the glucosamine and acetylglucosamine molecules are the constituents of the chitosan, it is worth to compare the theoretical spectra of these molecules with the experimental findings for chitosan. According to experimental data [30, 31], chitosan IR spectra range from 750 to 4000 cm^{-1} and three main regions of absorption, ~ 750 – 1700 cm^{-1} , 2850 – 3000 cm^{-1} , and 3100 – 3700 cm^{-1} . The vibrations of C-O-C group of ring mentioned above (1118 in A_Y , 1075 in A_X , and 1091 cm^{-1} in B) agree with 1050 cm^{-1} in chitosan [30]. The bending scissors vibration of NH_2 (1673 in A_Y , 1687 in A_X , and 1582 cm^{-1} in B), correspond to the band of 1559 cm^{-1} reported in [30], and 1594 cm^{-1} in [31]. The characteristic stretching vibrations of C-H bonds (2964 – 3066 in A_Y , 2915 – 3033 in A_X , and 2990 – 3063 cm^{-1} in B) correspond to 2800 – 2900 cm^{-1} in [30]. The vibration of 3450 cm^{-1} assigned to O-H stretching mode in [31] corresponds to the band 3449 cm^{-1} in B and assigned to the hydrogen bond stretching. In the similar region 3500 – 3600 cm^{-1} in A_Y , 3576 cm^{-1} in A_X , the vibrations are attributed to N-H stretching modes, while O-H stretching is observed at higher frequencies (3600 in A_Y , 3694 in A_X , 3977 cm^{-1} in B) than 3450 cm^{-1} reported in [31]. Except this discordance the theoretical findings for the glucosamine molecules A_Y , A_X , B demonstrate fair agreement of the characteristic frequencies of the functional groups with the experimental spectra of

chitosan.

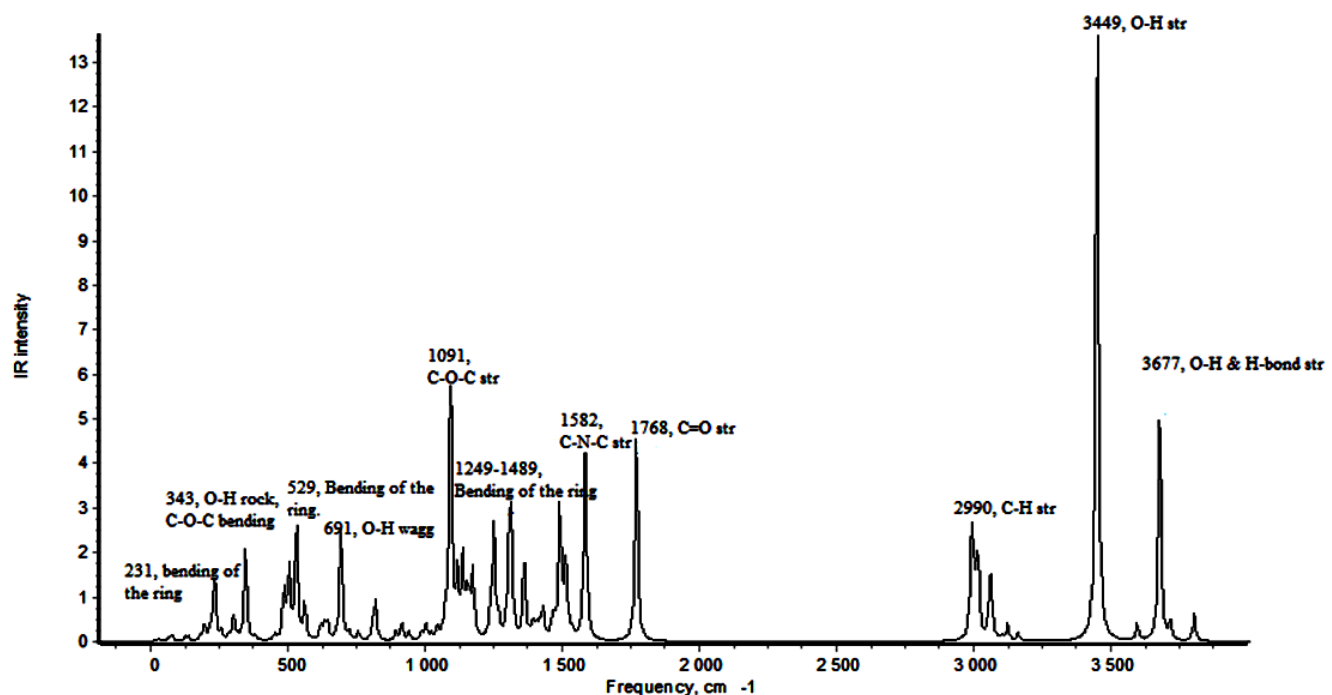


(a)

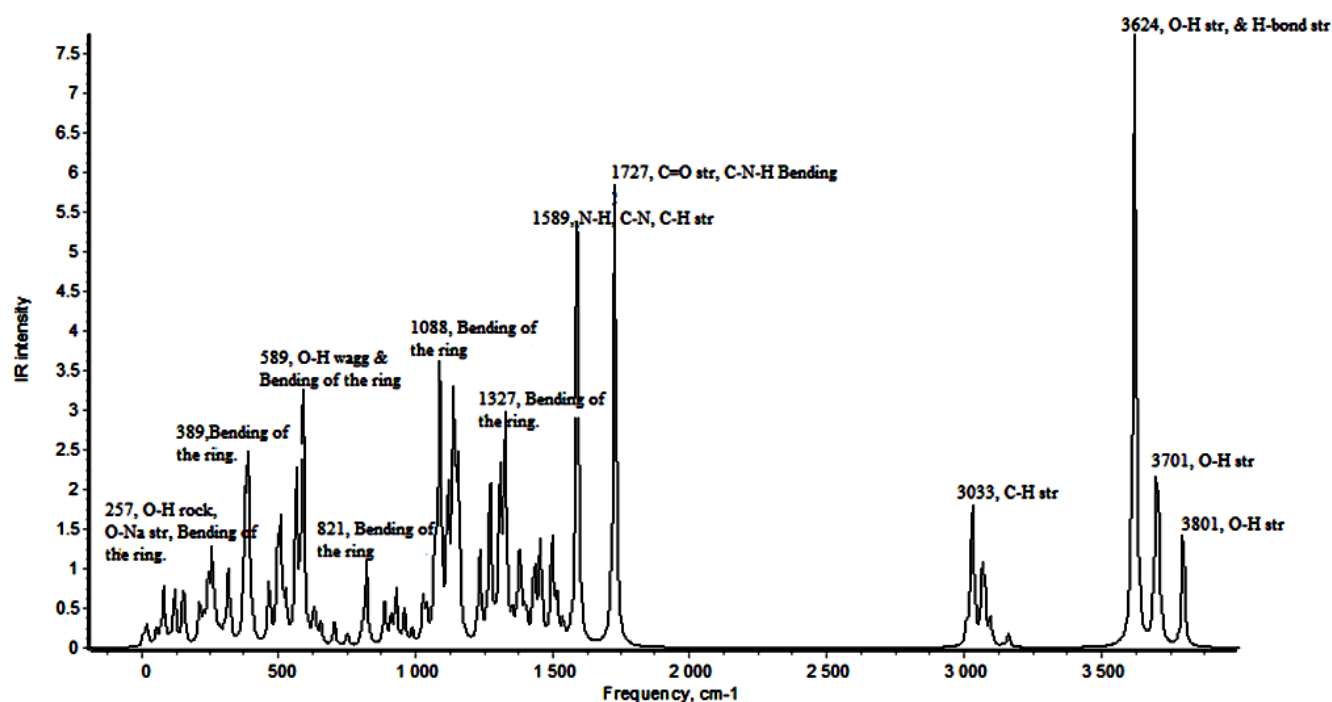


(b)

Figure 5. Theoretical IR spectra of glucosamine molecule A_x (a) and adduct $A_x\text{Na}^+$ (b).



(a)

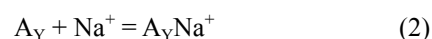
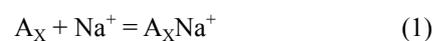


(b)

Figure 6. Theoretical IR spectrum of: acetylglucosamine B (a), adduct BNa^+ (b).

3.3. Thermodynamics of the Association Reactions

The thermodynamics of the reactions of Na^+ ion attachment to glucosamine and acetylglucosamine molecules is considered in this section. The reactions are as follows:



The energies of the reactions $\Delta_r E$ were found through the

total energy of the products and reactants:

$$\Delta_r E = E_{\text{prod}} - E_{\text{react}} \quad (4)$$

The enthalpies of reactions $\Delta_r H^\circ(0)$ were obtained using $\Delta_r E$, and the zero-point vibration energy corrections $\Delta ZPVE$ as given in following equations

$$\Delta_r H^\circ(0) = \Delta_r E + \Delta ZPVE \quad (5)$$

$$\Delta ZPVE = \frac{1}{2}hc (\Sigma\omega_{i \text{ prod}} - \Sigma\omega_{i \text{ react}}) \quad (6)$$

where h is the Plank's constant, c is the speed of light in the free space, $\Sigma\omega_{i \text{ prod}}$ and $\Sigma\omega_{i \text{ react}}$ are the sums of the vibration frequencies of the products and reactants, respectively.

The energies of the species were computed with basis set 6-31G(d) and also with more extended basis sets up to 6-311++G(d,p) under the fixed geometrical parameters optimized with 6-31G(d). Fig. 6 displays the calculated enthalpies of association reactions against different bases sets employed. The same trend is observed for the reactions (2) and (3), while for the reaction (1) the general trend is similar, but a discrepancy is seen for two cases: 6-311G(d,p) and 6-311++G(d,p). Nevertheless, the increase of values of $\Delta_r H^\circ(0)$ by $\sim 30\text{--}40 \text{ kJ}\cdot\text{mol}^{-1}$ with the extension of basis set from the lowest to the highest can be noticed.

Table 5. The reaction equations, energies $\Delta_r E$, zero point vibrational energy corrections $\Delta ZPVE$ and enthalpies $\Delta_r H^\circ(0)$ of the reactions; in $\text{kJ}\cdot\text{mol}^{-1}$.

N	Reaction	$-\Delta_r E$	$\Delta ZPVE$	$-\Delta_r H^\circ(0)$
1	$A_X + \text{Na}^+ = A_X\text{Na}^+$	201.9	6.2	195.7
2	$A_Y + \text{Na}^+ = A_Y\text{Na}^+$	234.5	7.1	227.4
3	$B + \text{Na}^+ = B\text{Na}^+$	234.0	4.9	229.2

The energies and enthalpies of the reactions obtained in the most extended basis set 6-311++G(d,p) are gathered in Table 5. Both for monomer A_Y and B, the enthalpies of the reactions are very close to each other, being equal to about $-228 \text{ kJ}\cdot\text{mol}^{-1}$

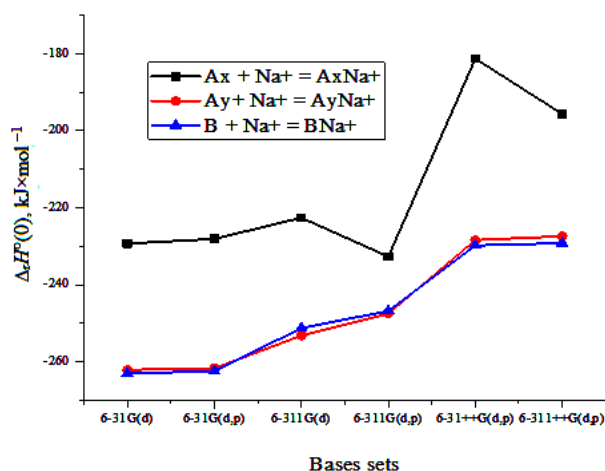


Figure 7. The calculated enthalpies of the reactions versus basis set.

¹ while for A_X the enthalpy is about $-196 \text{ kJ}\cdot\text{mol}^{-1}$. Therefore all three reactions are highly exothermic.

The Gibbs free energies $\Delta_r G^\circ(T)$ of reactions were calculated using the following equation

$$\Delta_r G^\circ(T) = \Delta_r H^\circ(T) - T\Delta_r S^\circ(T) \quad (7)$$

where $\Delta_r H^\circ(T)$ is the enthalpy of the reaction at temperature T , $\Delta_r S^\circ(T)$ is the change in entropy of the reaction. The thermodynamic functions of the A_X , A_Y , $A_X\text{Na}^+$, and $A_Y\text{Na}^+$, have been computed by the OpenThermo software [32], those for Na^+ gaseous ions are taken from [33]. The geometrical parameters and vibrational frequencies needed for the thermodynamic functions calculations have been obtained with 6-31G(d) basis set. To find the enthalpies $\Delta_r H^\circ(T)$, the enthalpy increments $H^\circ(T) - H^\circ(0)$ were used:

$$\Delta_r H^\circ(T) = \Delta_r H^\circ(0) + \Delta_r [H^\circ(T) - H^\circ(0)] \quad (8)$$

where the values of $\Delta_r H^\circ(0)$ were obtained with 6-311++G(d,p) basis set. The plot of the Gibbs free energies of reactions (1)-(3) is shown in Fig. 8. It can be seen, that the dependence for each reaction is close to linear. The reason of this behavior is due to slight change both in entropy $\Delta_r S^\circ(T)$ and enthalpy $\Delta_r H^\circ(T)$; for the latter the enthalpy increment $\Delta_r [H^\circ(T) - H^\circ(0)]$ is very small. The Gibbs energies grow due to the entropy factor $T\Delta_r S^\circ$, which is negative, increasing steadily in magnitude with temperature raise. The value of $\Delta_r G^\circ(T)$ are negative in a broad temperature range, this indicates that the association reactions are spontaneous. The negative values of $\Delta_r G^\circ$ relate mostly to exothermicity of the reactions. To the best of our knowledge, there is no information about existence of both glucosamine molecules and the adducts in vapour at elevated temperatures. But at moderate temperatures the adducts are thermodynamically stable.

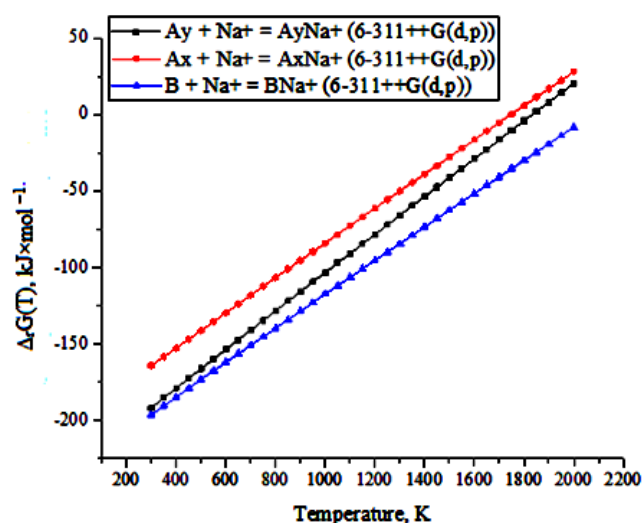


Figure 8. Gibbs free energies $\Delta_r G^\circ$ of the reactions against temperature.

4. Conclusion

The attachment of Na⁺ ion to the glucosamine (two conformers) and acetylglucosamine molecules has been studied by DFT/B3LYP method. The geometrical structure and vibrational spectra of the molecules and adducts with Na⁺ ion have been determined. It is revealed that the total energy of a conformer and adduct depends on the orientation of the functional groups OH and NH₂ regarding the carbon ring. The position of Na⁺ attachment is determined by both the atomic charges and mutual position of the atoms to interact: in the conformer A_Y it approaches the nitrogen and oxygen atoms, while in conformer A_X and acetylglucosamine B, the Na⁺ ion sticks to two oxygen atoms. The theoretical IR spectra of the molecules and adducts are reported, analyzed; and compared to the experimental findings for chitosan; the fair agreement of the characteristic vibrational modes in the molecules considered and chitosan have been observed. Thermodynamic characteristics of the attachment reactions between Na⁺ and the molecules have been determined. The exothermicity and spontaneous character of the adducts formation have been proved.

Acknowledgement

The authors are grateful to The Nelson Mandela African Institution of Science and Technology for the sponsorship. In a special way we acknowledge a valuable assistance and service by the School of Computational and Communication Science and Engineering.

References

- [1] A. L. Lehninger, "Principles of Biochemistry", *W.H. Freeman*, 4th edition, 2004.
- [2] R. Terreux, M. Domard, C. Viton, and A. Domard, "Interactions study between the copper II ion and constitutive elements of chitosan structure by DFT calculation," *Biomacromolecules*, vol. 7, pp. 31-37, 2006.
- [3] J. K. Chen, C. R. Shen, and C. L. Liu. "N-Acetylglucosamine: Production and applications". *Marine drugs* 8:9, 2010.
- [4] E. A. El-hefian, M. M. Nasef, and A. H. Yahaya., "Preparation and Characterization of Chitosan/Polyvinyl Alcohol Blends-A Rheological Study". *E-Journal of Chemistry* 7(S1):S349-S357, 2010.
- [5] C. E. Olteanu "Applications of Functionalized Chitosan". *Scientific study and Research* vol., VIII:(3). 2007.
- [6] G. Cardenas and S. P. Miranda, "FTIR and TGA studies of chitosan composite films," *Journal of the Chilean Chemical Society*, vol. 49, pp. 291-295, 2004
- [7] I. Uzun, and G. Topal. "Synthesis and Physicochemical Characterization of Chitin Derivatives". *Journal of Chemistry* 8, 2013.
- [8] N. M. Yahya., "Study the Effect of some Physical Parameters on the Diffusion Properties of Prepared Alginate-Chitosan Capsule". *Raf. J. Sci* 23:60-67, 2012.
- [9] M. Benavente, "Adsorption of metallic ions onto chitosan: equilibrium and kinetic studies," pp. 1654-1081, 2008.
- [10] H. Niu, and B. Volesky, "Characteristics of anionic metal species biosorption with waste crab shells". *Hydrometallurgy* 71(1-2):209-215, 2003.
- [11] G. Crini, N. Morin-Crini, N. Fatin-Rouge, S. Déon and P. Fievet, "Metal removal from aqueous media by polymer-assisted ultrafiltration with chitosan". *Arabian Journal of Chemistry* (2014), <http://dx.doi.org/10.1016/j.arabjc.2014.05.020>
- [12] R.A.A. Muzzarelli, "Chitins and chitosans for the repair of wounded skin, nerve, cartilage and bone". *Carbohydrate Polymers* 76:167-182, 2009.
- [13] A. Fattahi, M. Ghorat, A. Pourjavadi, M. Kurdtabar, and A. A. Torabi, "DFT/B3LYP Study of Thermochemistry of D-Glucosamine, a Representative Polyfunctional Bioorganic Compound," *Scientia Iranica*, vol. 15, pp. 422-429, 2008.
- [14] I. Aranaz, M. Mengibar, R. Harris, I. Paños, B. Miralles, N. Acosta, G. Galed, and Á. Heras, "Functional Characterization of Chitin and Chitosan". *Curr. Chem. Biol.* 3:203-230, 2009.
- [15] R.A.A. Muzzarelli, C. Jeunieux, and G.W. Gooday. "Chitin in Nature and Technology". *New York: Plenum Pres*, 1985.
- [16] Y. Luo, and Q. Wang. "Recent Advances of Chitosan and Its Derivatives for Novel Applications in Food Science". *journal of Food Processing and Beverages* 1, 2013.
- [17] J. Azimov, Sh. Mamatkulov, N. Turaeva, B. L. Oxengendler, and S. Sh. Rashidova, "Computer modeling of chitosan adsorption on a carbon nanotube". *J Struct Chem*, Vol. 53, No. 5, pp. 829-834, 2012.
- [18] R.A.A. Muzzarelli, "Potential of chitin/chitosan-bearing materials for uranium recovery: An interdisciplinary review". *Carbohydrate Polymers* 84:54-63, 2011.
- [19] A. D. Becke, "Perspective: Fifty years of density-functional theory in chemical physics". *The Journal of chemical physics* 140:18A301, 2014.
- [20] A. J. Cohen, P. Mori-Sánchez, and W. Yang, "Challenges for density functional theory". *Chem. Rev.* 112:289-320, 2011.
- [21] I. Peña, L. Kolesníková, C. Cabezas, C. Bermúdez, M. Berdakin, A. Simão, and J. L. Alonso, "The shape of D-glucosamine". *Phys. Chem. Chem. Phys.*, 16:23244, 2014.
- [22] I. Onoka, A. Pogrebnoi, T. Pogrebnya, "Geometrical Structure, Vibrational Spectra and Thermodynamic Properties of Chitosan Constituents by DFT Method". *International Journal of Materials Science and Applications*. Vol. 3, No. 4, 2014, pp. 121-128. doi: 10.11648/j.ijmsa.20140304.11
- [23] A. A. Granovsky, Firefly version 8.1.0, www, 2014 <http://classic.chem.msu.su/gran/firefly/index.html>.
- [24] M. W. Schmidt, K. K. Baldridge, J. A. Boatz, S. T. Elbert, M. S. Gordon, J. H. Jensen, S. Koseki, N. Matsunaga, K. A. Nguyen, S. Su, T. L. Windus, M. Dupuis, J. A. Montgomery. "General Atomic and Molecular Electronic Structure System". *J. Comput. Chem.* 1993; 14:1347-1363; doi:10.1002/jcc.540141112.
- [25] HyperChem^(TM), H., Inc., 1115 NW 4th Street, Gainesville, Florida 32601, USA.

- [26] B. M. Bode, and M. S. Gordon, MacMolPlt version 7.4.2. J. Mol. Graphics and Modeling, 1998; 16,133–138. Available: <http://www.scl.ameslab.gov/MacMolPlt/>.
- [27] Chemcraft. Version 1.7 (build 132). G.A. Zhurko, D.A. Zhurko. HTML: www.chemcraftprog.com.
- [28] M. Petrov, L. Lymperakis, M. Friák, and J. Neugebauer, "Ab Initio Based Conformational Study of the Crystalline α -Chitin". *Wiley periodicals, inc. Biopolymers*, 99:22-34,2013. DOI 10.1002/bip.22131
- [29] I. F. Amaral, P. L. Granja, and M. A. Barbosa. "Chemical modification of chitosan by phosphorylation: an XPS, FT-IR and SEM study",. *Journal of Biomaterials Science, Polymer Edition*, 16:1575-1593, 2005.
- [30] T. R. Sobahi, M. S. I. Makki, and M. Y. Abdelaal, "Carrier-mediated blends of Chitosan with polyvinyl chloride for different applications". *Journal of Saudi Chemical Society* 17:245-250, 2013.
- [31] S. Kunjachan, S. Jose, and T. Lammers, "Understanding the mechanism of ionic gelation for synthesis of chitosan nanoparticles using qualitative techniques," *Asian journal of pharmaceuticals*, vol. 4, p. 148, 2010.
- [32] K. Tokarev, "OpenThermo", v.1.0 Beta 1 (C) ed. <http://openthermo.software.informer.com/>, 2007-2009.
- [33] L. V. Gurvich, V. S. Yungman, G. A. Bergman, I. V. Veitz, A. V. Gusarov, V. S. Iorish, V. Y. Leonidov, V. A. Medvedev, G. V. Belov, N. M. Aristova, L. N. Gorokhov, O. V. Dorofeeva, Y. S. Ezhov, M.E. Efimov, N. S. Krivosheya, I. Nazarenko, E. L. Osina, V. G. Ryabova, P. I. Tolmach, N. E. Chandamirova, E.A.Shenyavskaya, "Thermodynamic Properties of individual Substances. Ivtanthermo for Windows Database on Thermodynamic Properties of Individual Substances and Thermodynamic Modeling Software", Version 3.0 (Glushko Thermocenter of RAS, Moscow, 1992-2000).